Small-Angle X-ray-Scattering Study of Supercritical Trifluoromethane

Keiko Nishikawa*

Department of Diversity Science, Graduate School of Science and Technology, Chiba University, Yayoi, Inage-ku, Chiba 263, Japan

Takeshi Morita

Department of Chemistry, Faculty of Education, Yokohama National University, Tokiwadai, Hodogaya-ku, Yokohama 240, Japan

Received: October 7, 1996; In Final Form: December 12, 1996[⊗]

Small-angle X-ray-scattering experiments for supercritical CF_3H were carried out. As in the previous results for supercritical CO_2, the correlation lengths and density fluctuations for CF_3H form a ridge along the extension of the coexistence curve of gas and liquid when the contour maps of their values are drawn in the $P-T$ phase diagram. However, the ridges of the two samples do not overlap perfectly with each other in the diagram. The extension curves correspond to the loci of the phase transition with higher order.

Introduction

Supercritical fluids have attracted much interest as promising solvents because their properties can be changed drastically with small changes in control variables such as temperature and pressure. It is said that the characteristic properties of supercritical fluids as solvents are caused by the ability of clustering around the solute molecules.[1−6] As well as solutions, the solvent molecules themselves tend to aggregate or form "clusters" in their supercritical state.[7−11] This ability of clustering in pure supercritical fluids seems to have a great influence on the structure and properties of the solution systems.

The present authors studied the clustering of supercritical CO_2 by small-angle X-ray-scattering (SAXS) experiments and reported the density fluctuations and correlation lengths at various thermodynamic states as a measure of the formation of clusters. It was shown that the density fluctuations and the correlation lengths form a ridge along the extension of coexistence curve of gas and liquid when the contour maps of their values are drawn in the phase diagram of pressure *vs* temperature.[10,11] This tendency has been related to the characteristic properties of the supercritical solutions;[10,11] that is, the rate of solubility and the rate constants of various reactions in supercritical CO_2 show singular behavior on the extension curve. The extension curve nearly corresponds to the critical isochore.

The same behavior was observed in other supercritical fluids. For example, the isothermal compressibility κ_T (this value is proportional to the density fluctuation) of supercritical Ar has the maximum value on the extension curve.[7] In other supercritical solvents beside CO_2, chemical reactions also exhibit anomalies on the curve.[12−15]

Therefore, the tendency mentioned above seems to be the general behavior for supercritical fluids. In order to confirm the properties in density fluctuation and correlation length of supercritical states, SAXS experiments are made for supercritical CF_3H in the present study. Molecules of CF_3H interact with each other by a very strong dipole moment. On the other hand, a molecule of CO_2 has quadrapole moment. It is interesting to know whether or not the difference of the molecular interaction causes any difference in the behaviors of the supercritical fluids mentioned above.

In the previous study, we expressed ambiguously that the locus where the density fluctuations and the correlation lengths take maximum values is on the extension curve of the coexistence curve of gas and liquid.[10,11] Another purpose of the present study is to determine the extension curve precisely in the phase diagram and to discuss it in relation to the critical isochore.

Experimental Section

Construction of Sample Holder. In the previous experiments,[10,11] the sample holder with Be windows[16] was used. However, Be gave very strong scattering in the small *s*-region ($s = (4\pi \sin\theta)/\lambda$; 2θ, scattering angle; λ, wavelength of X-ray) due to the mosaic structure, which prevented the accurate measurements of scattering intensities up to the smaller *s*-region. Therefore, we have constructed a sample holder with diamond windows suitable to SAXS measurements of supercritical fluids.

The cross sections of the sample holder are shown in Figure 1. The body is made of SUS316. The part marked with hatches is filled with the sample. The windows are made of diamond disks with a (100) plane which are 4 mm in diameter and 0.4 mm in thickness (dotted part in Figure 1). The diamond disks press tightly to the stainless body which is grinded in mirror planes, and there is no leakage when a high-pressure sample is contained in the holder. The attenuation due to absorption by the windows for X-rays of 1.5 Å wavelength is about 30%. The holder endured pressures up to 15 MPa.

The temperature of the sample is kept constant by flowing temperature-controlled water through a jacket of the sample holder. It is possible to set the temperature of the sample in the range of 0−60 °C. The temperature and pressure of the sample are monitored by means of an alumel-chromel thermocouple and a strain gauge. The construction of the holder was carried out by Hikari-Kouatsu Co. Ltd.

Measurements. Scattering experiments were carried out at BL-15 station, Photon Factory at National Laboratory for High Energy Physics, Tsukuba, using a SAXS apparatus constructed at the station.[17,18] By a bent mirror and a bent monochrometer made of Si single crystal, X-rays of 1.5 Å wavelength were selected and the beam was focused to 1.2×0.8 mm^2 at the position sensitive proportional counter (PSPC). The camera length was 2400 mm, and the X-ray path was evacuated except at the position where the sample holder was set.

[⊗] Abstract published in *Advance ACS Abstracts,* February 1, 1997.

S1089-5647(96)03075-1 CCC: $14.00

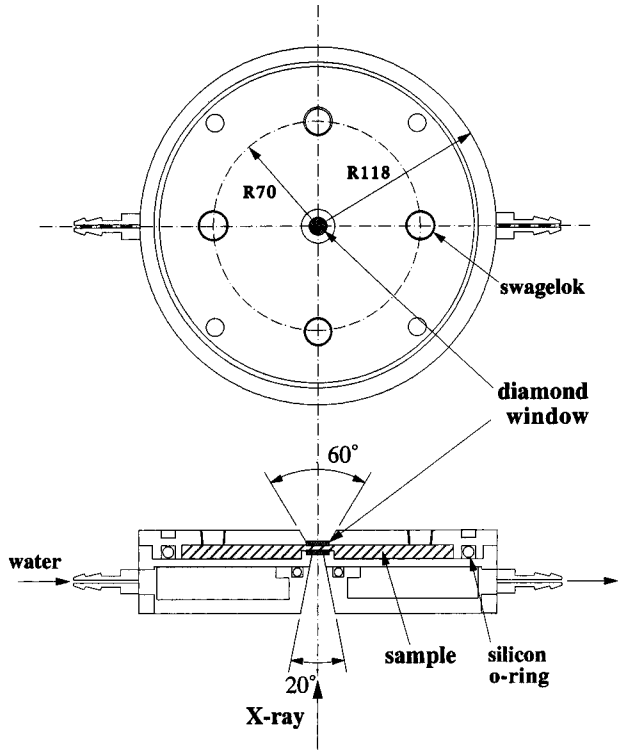

Figure 1. Cross section of the sample holder.

TABLE 1: Correlation Lengths and Density Fluctuations of the Thermodynamic States of CF_3H Investigated in the Present SAXS Experiments

	temp/K	pressure/ MPa	density/ g cm^{-3} [a]	ρ/ρ_c	ξ/Å	$\langle(\Delta N)^2\rangle/N$ exptl	$\langle(\Delta N)^2\rangle/N$ calcd
CP	299.06	4.836	0.525				
a	315.0 (±0.0)	9.29 (±0.00)	0.792	1.51	5.78	2.77	1.84
b	315.8 (±0.0)	8.29 (±0.00)	0.717	1.37	7.04	3.30	3.14
c	315.7 (±0.2)	7.56 (±0.00)	0.640	1.22	8.83	5.49	5.23
d	310.8 (±0.1)	7.09 (±0.02)	0.695	1.32	8.40	3.69	4.79
e	310.8 (±0.1)	6.88 (±0.01)	0.664	1.27	9.34	5.76	6.11
f	310.9 (±0.2)	6.65 (±0.02)	0.593	1.13	10.69	7.31	8.32
g	311.1 (±0.2)	6.41 (±0.03)	0.546	1.04	12.65	11.29	10.97
h	311.1 (±0.0)	6.17 (±0.00)	0.472	0.90	13.13	12.95	11.43
i	311.0 (±0.1)	5.86 (±0.00)	0.388	0.74	10.44	8.78	9.07
j	310.8 (±0.2)	5.50 (±0.01)	0.316	0.60	7.47	4.63	6.38
k	311.5 (±0.1)	6.09 (±0.01)	0.436	0.83	11.85	11.22	10.32
l	315.5 (±0.1)	6.51 (±0.01)	0.441	0.84	10.01	8.37	8.09
m	305.3 (±0.1)	5.47 (±0.01)	0.429	0.82	16.70	20.69	17.88
n	300.2 (±0.0)	4.91 (±0.00)	0.366	0.70	24.48	37.42	19.66
o	300.3 (±0.1)	5.06 (±0.01)	0.647	1.23	12.80	8.86	36.81
P	300.4 (±0.0)	5.36 (±0.01)	0.746	1.42	9.16	5.02	6.31
q	300.3 (±0.1)	5.78 (±0.01)	0.800	1.52	7.26	3.22	3.20
r	310.9 (±0.1)	5.18 (±0.00)	0.268	0.51	6.07	2.98	4.76
s	316.1 (±0.0)	6.30 (±0.01)	0.388	0.74	8.71	6.40	6.95
t	316.0 (±0.1)	5.85 (±0.01)	0.316	0.60	6.79	3.92	5.28

[a] Calculated using the equation of state for CF_3H.[20]

A beam stopper is made of lead. A hole is bored at the center of the stopper, at which a copper disk of 0.4 mm thickness is placed. The direct beam passes through the disk, and the resulting attenuated beam reaches the PSPC. By measuring the attenuated intensity of the direct beam for the case that the sample is in the holder and the one for the case that the holder is empty, the absorption factor μl by the sample (μ, the linear absorption coefficient of the sample; l, the path length of the sample) can be obtained experimentally. For all the samples the absorption factors were determined in this way.

The critical constants of CF_3H are 4.84 MPa, 299.1 K, and 0.525 g cm^{-3}. The SAXS intensities were measured for 20 thermodynamic states of supercritical CF_3H. Their thermodynamic data are listed in Table 1 and shown in the pressure *vs* temperature phase diagram (Figure 2).

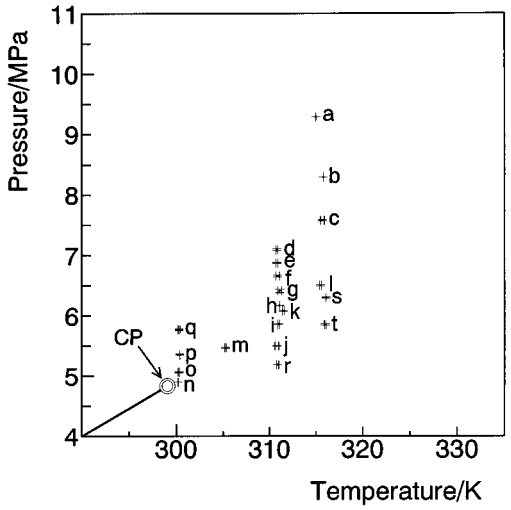

Figure 2. Measured thermodynamic states of CF_3H. The critical point is denoted as CP. The widths of the data points show the fluctuations of temperature and pressure.

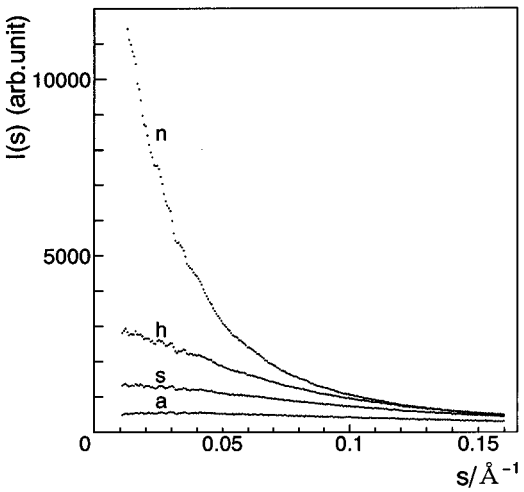

Figure 3. Intensities of small-angle X-ray scattering for typical thermodynamic state of CF_3H (states a, h, n, and s).

The accumulation time for an intensity measurement of each sample was 10 min. During the measurement, the pressure and the temperature were kept constant within the range of 0.02 MPa and 0.1 K, respectively, as listed in Table1. There is no leakage of the sample during each measurement. The fluctuations of the pressure were due to the temperature derivation of the sample. The observable s-value was $s = 0.01-0.22$ Å^{-1} by use of the SAXS apparatus at BL-15A and the constructed sample holder with diamond windows, while the measurable minimum s-value was 0.036 for the sample holder with Be windows.[10,11] The adoption of the diamond windows made it possible to measure the scattering intensity up to smaller s-region.

Various corrections for the observed scattering intensities were made, *i.e.*, the subtraction of instrumental backgrounds, the absorption correction, and the correction for the fluctuation of the beam intensity.

Results and Discussion

The scattering intensities for several thermodynamic states (a, h, n, and s) obtained after the corrections are shown in Figure 3. According to the Ornstein−Zernike theory for the samples

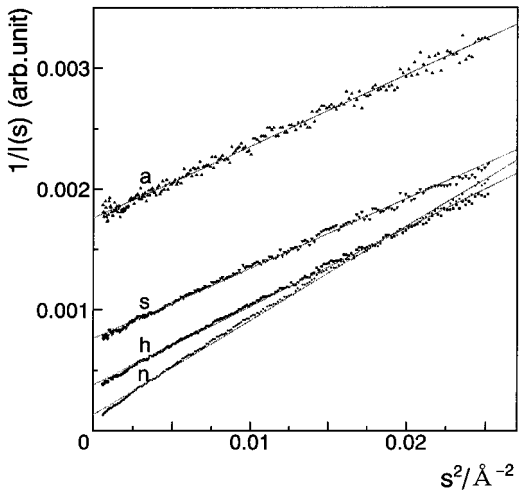

Figure 4. Ornstein−Zernike plots for states a, h, n, and s.

near the critical point, the scattering intensity near $s = 0$ is given by[19]

$$I(s) = \frac{I(0)}{(1 + \xi^2 s^2)} \tag{1}$$

where ξ is the Ornstein−Zernike correlation length and $I(0)$ is the scattering intensity at $s = 0$ (zero-angle scattering intensity). The so-called Ornstein−Zernike plots of $1/I(s)$ *vs* s^2 for the present CF_3H data form straight lines except the state n, as shown in Figure 4. This discrepancy from the straight line for the state n seems to be because the state is very near the critical point. In all the other thermodynamic states, the Ornstein−Zernike regime was shown to be operative.

The parameters obtained from each Ornstein−Zernike plot, *i.e.*, $1/I(0)$ and $\xi^2/I(0)$, are in arbitrary units. The values in absolute scale were obtained by the following procedure. The zero-angle scattering intensity normalized to that per molecule, $I(0)/N$, is related to the density fluctuation, $\langle(\Delta N)^2\rangle/N$, as

$$I(0)/N = Z^2\langle(\Delta N)^2\rangle/N \tag{2}$$

where Z is the number of electrons in a molecule and N is the number of molecules in the corresponding volume V. The density fluctuation can be also estimated by the isothermal compressibility κ_T as

$$\langle(\Delta N)^2\rangle/N = (N/V)\kappa_T k_B T \tag{3}$$

where k_B is the Boltzmann constant and T is the thermodynamic temperature.[19] The κ_T values in the supercritical states of CF_3H were calculated using the state equation given by Aizpiri *et al.*[20] The scaling factor to normalize the experimental intensities to the absolute scale was obtained by use of four data points (a, b, d, and q) through the relations of eqs 2 and 3. Others were corrected to the absolute scale by multiplying the scaling factor. The correlation lengths and the density fluctuations thus obtained by the present SAXS experiments are listed in Table 1, with the density fluctuations calculated from the state equation. The agreement of the values of the density fluctuation by the SAXS experiment with the calculated ones is fairly good except the data points of the isothermal condition of 300.3 K (n, o, and p). The temperatures for the data points n, o, and p are very near the critical one. Errors of even 0.01 MPa or 0.1 K cause a large difference of the state. This is the one of the origins for the difference of the experimental and calculated values. The values obtained from the Ornstein−Zernike plot give us

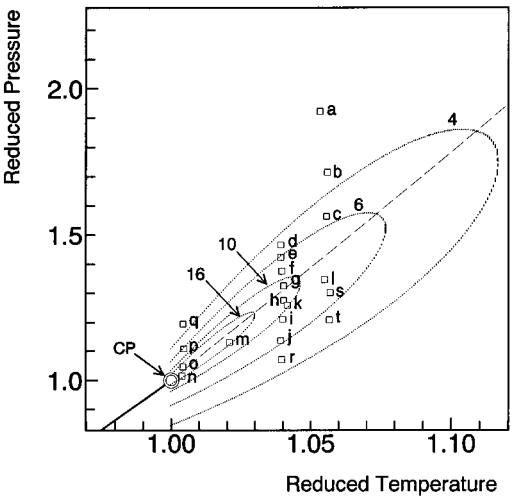

Figure 5. Measured points for CF_3H and the contour lines of the density fluctuation $\langle(\Delta N)^2\rangle/N$ drawn on the reduced pressure (P/P_c) *vs* the reduced temperature (T/T_c) diagram. The numbers on the lines represent their values. The broken curve is the locus of the states with the same density as the critical one.

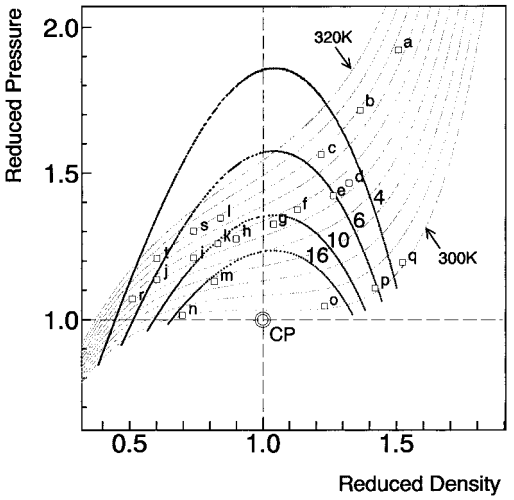

Figure 6. Measured points for CF_3H and contour lines of the density fluctuation $\langle(\Delta N)^2\rangle/N$ drawn on the reduced pressure (P/P_c) *vs* the reduced density (ρ/ρ_c) diagram. The numbers on the lines represent their values.

direct information on the size distribution of clusters and the inhomogeneity of the distribution of molecules.

In the results for CO_2,[10,11] it was reported that the density fluctuation $\langle(\Delta N)^2\rangle/N$ and the correlation length ξ have large values along the extension of the coexistence curve of gas and liquid (hereafter called "the extension curve"). The present data for CF_3H are shown in $P-T$ plane (Figure 5) and in $P-\rho$ plane (Figure 6). In order to compare the present results with the ones for CO_2 later, pressure, temperature, and density are described as the reduced values. The dotted curves in Figure 5 and 6 are contour lines of the values of the density fluctuation which are obtained by the calculated κ_T values. The numbers on the curves represent their values. The values of the density fluctuation determined by the present SAXS experiment are in the same tendency as in the calculated contour map (see Table 1). As shown in Figure 5, the density fluctuation for CF_3H forms a ridge along the extension curve as well as for CO_2. The broken curve in Figure 5 is the locus of the states with the same density as the critical density; namely, the curve corresponds to the critical isochore. The critical isochore differs slightly from the ridge of the density fluctuation. The difference becomes large, as the states are far from the critical point. This

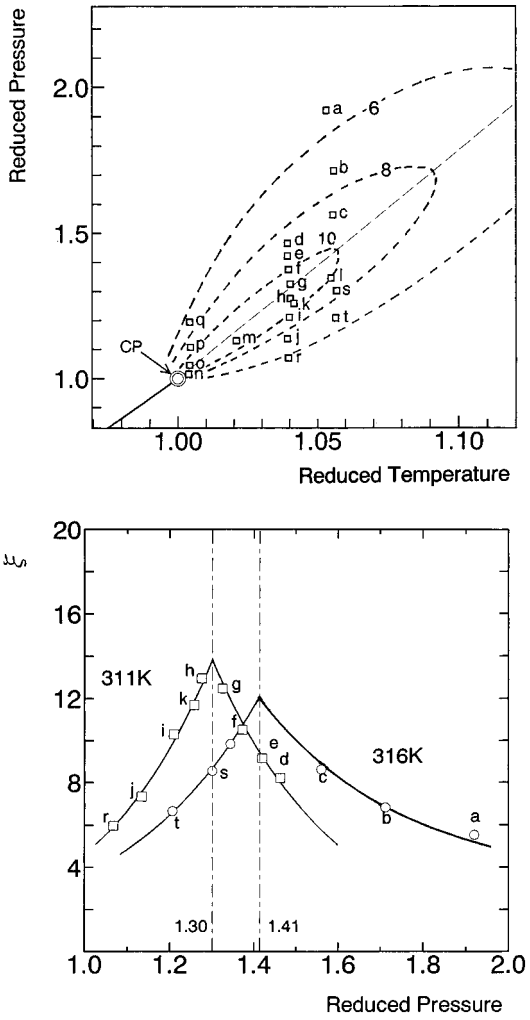

Figure 7. Contour lines of the correlation lengths for CF_3H. The numbers on the lines represent their values in angstroms. The thin broken line is the critical isochore. (b). Correlation lengths *vs* reduced pressure in isothermal conditions (311 and 316 K).

behavior is also seen in the case of CO_2 supercritical states.[10,11] In the previous papers, we said the ridge roughly refers to the critical isochore. However, strictly speaking, the ridge slightly slides from the critical isochore and the density at which the density fluctuation reaches a maximum deviates gradually from the ρ_c as the temperature increases, which is pointed out by Gray *et al.*[21]

For the correlation length for CF_3H, the contour map in the pressure *vs* temperature phase diagram is shown in Figure 7a. The ridge where the correlation lengths take maxima is also along a extension curve. However, the ridge for the correlation length does not seem to overlap perfectly with the one for the density fluctuation. Figure 7b shows the pressure dependence of the correlation length in isothermal conditions (311 and 316 K). The reduced pressures of the peak positions are 1.30 and 1.41, respectively, corresponding to the values determined by the cross-points of the critical isochore and the isothermal lines. It is difficult to discuss the details of the contour map for the correlation length, because the correlation length is determined experimentally only by the diffraction methods and the measured points of the present study are not enough to draw the contour map precisely. However, as seen from Figure 7b, we conclude that the ridge for the correlation length differs from the one for the density fluctuation and the former is nearly equal to the critical isochore.

The plots of the logarithm of the density fluctuations against the logarithm of the correlation lengths are shown in Figure 8.

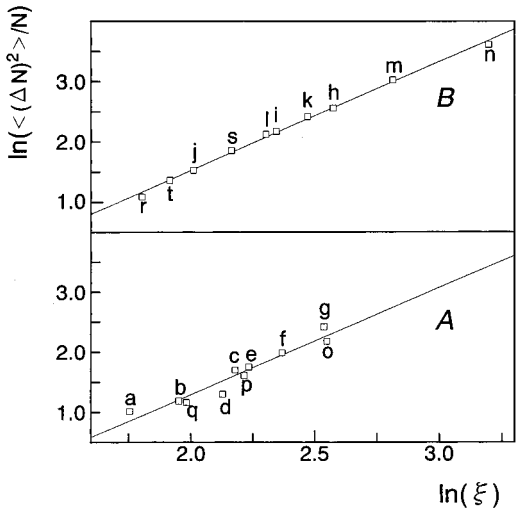

Figure 8. Plots of the logarithm of the density fluctuations against the logarithm of the correlation lengths. Points form two straight lines. Line A is constituted by the states in the higher-density region. Line B is constituted by the states in the lower-density region.

As well as the results of CO_2,[10,11] the plots form two straight lines. The one (line A) is constituted by the states in the upper side of the ridge (in the higher-density region) in Figure 5. The other is a line (line B) which is composed of the states in the bottom side of the ridge (in the lower-density region). Least-squares fittings for line A give

$$\ln(\langle(\Delta N)^2\rangle/N) = 1.78(\ln \xi) - 2.26 \tag{4}$$

and for line B

$$\ln(\langle(\Delta N)^2\rangle/N) = 1.81(\ln \xi) - 2.09 \tag{5}$$

The standard deviations for the values of the inclinations 1.78 and 1.81 are 0.11 and 0.03, respectively.

In the critical-point exponents analyses,[19] the values of κ_T and ξ are described by

$$\kappa_T \sim \epsilon^{-\gamma} \tag{6}$$

and

$$\xi \sim \epsilon^{-\nu} \tag{7}$$

where

$$\epsilon = (T - T_c)/T_c \tag{8}$$

Though the absolute values of γ and ν are different, depending on the models or approximations used, the ratio γ/ν is always 2.0 for all the models.[19] As shown by eq 3, the density fluctuation $\langle(\Delta N)^2\rangle/N$ is proportional to κ_T. Therefore, the inclination of $\ln(\langle(\Delta N)^2\rangle/N)$ *vs* $\ln(\xi)$ corresponds to γ/ν. In the case of the SAXS results for CO_2, the values also becomes 2.0 within the experimental error.[11] The value about 1.8 in the present study for CF_3H differs from the value by the model calculations and the CO_2 results. It is not clear whether the origin of the discrepancy comes from the experimental error or from the character dependent on the sample. The experimental conditions for CF_3H were better than the ones for CO_2,[11] and the accuracy of the obtained value in the present study seems better than the latter one. The present sample, a CF_3H molecule, has a strong dipole moment. It may be possible to say that the very strong molecular interaction causes the discrepancy from the exponent rule. However, in order to get a definite

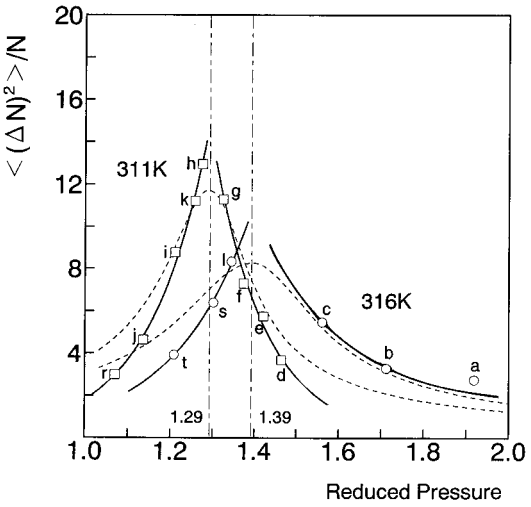

Figure 9. Density fluctuations *vs* reduced pressure in isothermal conditions (311 and 316 K). The squares and circles are the present experimental results, and broken curves are the calculated results by the use of the state equation Aizpiri *et al.*[20]

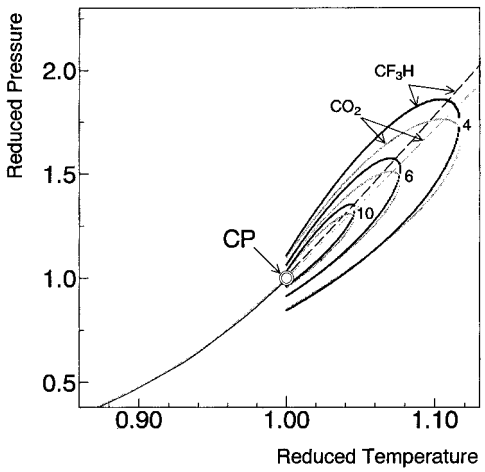

Figure 10. Comparison of the contour maps of the density fluctuation for CF_3H (dark lines) and for CO_2 (light lines). The numbers on the curve represent the values. Broken lines are the critical isochores.

conclusion, experimental studies for other samples with strong molecular interactions are necessary.

The same as the CO_2 case, within the experimental error, it is possible to say that line A is parallel to line B; namely, the two lines will cross at infinity. The cross-point of the two lines corresponds to the critical point.

Equations 4 and 5 show that the dependence of the density fluctuation on the correlation length is different across the boundary of the extension curve. As pointed out in the previous paper for supercritical CO_2,[10,11] the several variables related to the second derivatives of the Gibbs energy, such as isothermal compressibility, density fluctuations, and partial molar volumes in solution systems at infinite dilution of solutes, become maximum or minimum on the extension curve. We maintained that the extension curve corresponds to the locus of the phase transition with higher order than the second. In the present results for CF_3H, the large change of the values across the ridge of the density fluctuation is well shown in Figure 9. Figure 9 shows the pressure dependence of the density fluctuations in isothermal conditions (311 and 316 K). The points (squares and circles) are the experimental results, and the broken curves are the calculated values from the state equation.[20] The experimental data form λ-shaped peaks, whereas the calculated values form symmetrical smooth peaks. This may be because the empirical equation of the state cannot describe the anomaly on the locus of the higher-order phase transition. Although the shapes of the peaks by calculated values are slightly different from the ones obtained by experimental values, the peak positions are the same for the two cases. The peaks are positioned at 1.29 and 1.39 in the reduced pressure for isothermal measurements, whose values correspond to the ones determined by the cross-points of the ridge for the density fluctuation and the isothermal lines and are not the reduced pressures on the critical isochore. As found by the experimental results of the SAXS for CO_2 and CF_3H, the ridge for the density fluctuation is the boundary which separates the supercritical states. It may be possible to say that the states on the upper side of the boundary (the higher-density region) in Figure 5 are more liquidlike and the ones on the bottom side (the lower density region) are more gaslike.

The contour maps of the calculated density fluctuation for CF_3H and CO_2 are figured in the same phase diagram (Figure 10). The dark lines correspond to the the map for CF_3H, and the light ones correspond to CO_2. For CO_2, the density fluctuations were calculated by use of the state equation by Huang *et al.*[22] The two broken curves are critical isochores. The full line is the coexistence curve of gas and liquid and it is well-known that the coexistence curves form the same curves independent of the substances when they are figured on the phase diagram with the reduced variables. As seen in Figure 10, the critical isochores of CF_3H and CO_2 do not overlap perfectly each other in the $P-T$ phase diagram. The contour maps do not overlap each other, either. The volumes of CO_2 and CF_3H molecules differ; the molecular interaction for the former is the quadrapole moment, and the one for the latter is a very strong dipole moment. It is interesting to study how the locus of the phase transition with the higher order is figured in the phase diagram dependent on the substances. Figure 10 was obtained by the calculation using the empirical state equations.[20,22] In order to discuss the locus of the higher-order phase transition in supercritical regions, it is necessary to discuss the accuracy of the state equations and moreover to carry out to precise SAXS measurement for more thermodynamic states. The perfect answer for the the discussion mentioned above is beyond the scope of the present paper and shall be left to future investigations.

In conclusion, the density fluctuations for supercritical CF_3H form a ridge along the extension of the coexistence curve of gas and liquid, which is slightly different from the critical isochore, is the case for CO_2. The correlation lengths also from a ridge. However, this ridge nearly overlaps to the critical isochore. The ridge of the density fluctuations corresponds to the locus of the phase transition with higher order. The contour maps of the density fluctuations for CF_3H and CO_2 do not overlap with each other, which seems to show the substance dependence of the density fluctuations.

Acknowledgment. The authors thank Dr. Yoshiyuki Amemiya, KEK, for his guidance on the experiments at Photon Factory, KEK. This work has been supported by a Grant-in-Aid for Scientific Research on Priority Areas from the Ministry of Education, Science and Culture.

References and Notes

(1) Kim, S; Johnston, K. P. *Ind. Eng. Chem. Res.* **1987**, *26*, 1206.
(2) Debenedetti, P. G. *Chem. Eng. Sci.* **1987**, *42*, 2203.
(3) Petsche, I. B.; Debenedetti, P. G. *J. Chem. Phys.* **1989**, *91*, 7075.
(4) Kajimoto, O; Futakami, M.; Kobayashi, T.; Yamasaki, K. *J. Phys. Chem.* **1988**, *92*, 1347.
(5) Morita, A.; Kajimoto, O. *J. Phys. Chem.* **1990**, *94*, 6420.

(6) Chialvo, A. A.; Debenedetti, P. G. *Ind. Eng. Chem. Res.* **1992**, *31*, 1391.
(7) Thomas, J. E.; Schmidt, V. M. *J. Chem. Phys.* **1963**, *39*, 2506.
(8) Londono, J. D.; Shah, V. M.; Wignall, G. D.; Cochran, H. D.; Bienkowski, P. R. *J. Chem. Phys.* **1993**, *99*, 466.
(9) Nishikawa, K.; Takematsu, M. *Chem. Phys. Lett.* **1994**, *226*, 359.
(10) Nishikawa, K.; Tanaka, I. *Chem. Phys. Lett.* **1995**, *244*, 149.
(11) Nishikawa, K.; Tanaka, I.; Amemiya, Y. *J. Phys. Chem.* **1996**, *100*, 418.
(12) Otto, B.; Schroeder, J.; Troe, J. *J. Chem. Phys.* **1984**, *81*, 202.
(13) Simmons, G. M.; Mason, D. M. *Chem. Eng. Sci.* **1972**, *27*, 89.
(14) Kimura, Y.; Yoshimura, Y.; Nakahara, M. *J. Chem. Phys.* **1989**, *90*, 5679.
(15) Kimura, Y.; Yoshimura, Y. *J. Chem. Phys.* **1992**, *96*, 3085, 3824.
(16) Nishikawa, K.; Takematsu, M. *Jpn. J. Appl. Phys.* **1993**, *32*, 5155.
(17) Amemiya, Y; Wakabayashi, K.; Hamanaka, T.; Wakabayashi, T.; Matsushita, T.; Hashizume, H. *Nucl. Instrum. Methods* **1983**, *208*, 471.
(18) Wakabayashi, K.; Amemiya,Y. In *Handbook on Synchrotron Radiation*; Ebashi, S., Koch, M., Rubinstein, E., Eds.; North-Holland: Amsterdam, 1991; Chapter 19.
(19) Stanley, H. E. *Introduction to Phase Transitions and Critical Phenomena*; Oxford University Press: Oxford, 1971.
(20) Aizpiri, A. G.; Rey, A.; Davila, J.; Rubio, R. G.; Zollweg, J. A.; Streett, B. *J. Phys. Chem.* **1991**, *95*, 3351.
(21) Gray C. G.; Goldman, S.; Tomberli, B.; Li, W. *Chem Phys. Lett.*, in press.
(22) Huang, F. H.; Li, M. H.; Lee, L. L.; Staling, K. E.; Chung, F. T. H. *J. Chem. Eng. Jpn.* **1985**, *18*, 490.